The MAXI Mission on the ISS: Science and Instruments for Monitoring All-Sky X-Ray Images

Masaru Matsuoka,[1] Kazuyoshi Kawasaki,[1] Shiro Ueno,[1] Hiroshi Tomida,[1] Mitsuhiro Kohama,[1,2] Motoko Suzuki,[1]
Yasuki Adachi,[1] Masaki Ishikawa,[1] Tatehiro Mihara,[2] Mutsumi Sugizaki,[2] Naoki Isobe,[2] Yujin Nakagawa,[2]
Hiroshi Tsunemi,[3] Emi Miyata,[3] Nobuyuki Kawai,[4] Jun Kataoka,[4]* Mikio Morii,[4] Atsumasa Yoshida,[5]
Hitoshi Negoro,[6] Motoki Nakajima,[6] Yoshihiro Ueda,[7] Hirotaka Chujo,[2] Kazutaka Yamaoka,[5]
Osamu Yamazaki,[5] Satoshi Nakahira,[5] Tetsuya You,[5] Ryoji Ishiwata,[6] Sho Miyoshi,[6]
Satoshi Eguchi,[7] Kazuo Hiroi,[7] Haruyoshi Katayama,[8] and Ken Ebisawa[9]

[1]*ISS Science Project Office, ISAS, JAXA, 2-1-1 Sengen, Tsukuba, Ibaraki 305-8505*
matsuoka.masaru@jaxa.jp
[2]*Cosmic Radiation Laboratory, RIKEN, 2-1 Hirosawa, Wako, Saitama 351–198*
[3]*Department of Earth and Space Science, Osaka University , 1-1 Machikaneyama, Toyonaka, Osaka 560-0043*
[4]*Department of Physics, Tokyo Institute of Technology, 2-12-1 Ookayama, Meguro-ku, Tokyo 152-8551*
[5]*Department of Physics and Mathematics, Aoyama Gakuin University, 5-10-1 Fuchinobe, Sagamihara, Kanagawa 229-8558*
[6]*Department of Physics, Nihon University, 1-8-14, Kanda-Surugadai, Chiyoda-ku, Tokyo 101-8308*
[7]*Department of Astronomy, Kyoto University, Oiwake-cho, Sakyo-ku, Kyoto 606-8502*
[8]*Earth Observation Research Center, JAXA, 2-1-1 Sengen, Tsukuba, Ibaraki 305-8505*
[9]*Institute of Space and Astronautical Science, JAXA, 3-1-1 Yoshinodai, Sagamihara, Kanagawa 229-8510*

Abstract

The Monitor of All-sky X-ray Image (MAXI) mission is the first astronomical payload to be installed on the Japanese Experiment Module — Exposed Facility (JEM-EF or Kibo-EF) on the International Space Station. It has two types of X-ray slit cameras with wide FOVs and two kinds of X-ray detectors consisting of gas proportional counters covering the energy range of 2 to 30 keV and X-ray CCDs covering the energy range of 0.5 to 12 keV. MAXI will be more powerful than any previous X-ray All Sky Monitor payloads, being able to monitor hundreds of Active Galactic Nuclei. A realistic simulation under optimal observation conditions suggests that MAXI will provide all-sky images of X-ray sources of ~ 20 mCrab ($\sim 7 \times 10^{-10}$ erg cm^{-2} s^{-1} in the energy band of 2–30 keV) from observations during one ISS orbit (90 min), ~ 4.5 mCrab for one day, and ~ 2 mCrab for one week. The final detectability of MAXI could be ~ 0.2 mCrab for two years, which is comparable to the source confusion limit of the MAXI field of view (FOV). The MAXI objectives are: (1) to alert the community to X-ray novae and transient X-ray sources, (2) to monitor long-term variabilities of X-ray sources, (3) to stimulate multi-wavelength observations of variable objects, (4) to create unbiased X-ray source catalogues, and (5) to observe diffuse cosmic X-ray emissions, especially with better energy resolution for soft X-rays down to 0.5 keV.

Key words: catalogs: X-ray source catalogue — instrumentation: All Sky Monitor (ASM) — stars: X-ray novae — stars: X-ray transients — X-ray: AGN — X-ray: GRB

1. Introduction

All Sky Monitors (ASMs) for X-ray observations have a long history (Holt & Priedhorsky 1987). The ASM aboard Ariel 5 (a British satellite) was the first dedicated pioneer payload to observe X-ray novae and transients (Holt 1976). The Ariel 5 ASM, which has two sets of one-dimensional scanning pinhole cameras, discovered several novae and transient X-ray objects. Thereafter, the terms "X-ray nova" and "X-ray transient" have become well-known in X-ray astronomy. X-ray instruments with a wide field of view (FOV) as well as ASM can not only detect X-ray novae and transients, but also monitor long-term X-ray variabilities of X-ray sources (Priedhorsky & Holt 1987).

Although Vela A & B satellites with a wide FOV discovered the first gamma-ray burst (GRB) before the Ariel-ASM (Klebesadel et al. 1973), those detectors were not very suitable for monitoring GRBs as well as X-ray novae and transients. Subsequently, dedicated GRB monitors confirmed that a considerable number of mysterious GRBs are produced in the universe. GRB monitors with a wide FOV have advanced greatly since a wide-field camera aboard Beppo-SAX discovered a GRB afterglow (Costa et al. 1997). Since then, special GRB satellites, such as HETE-2 (Ricker et al. 2002; Shirasaki et al. 2003) and Swift (Gehrels et al. 2004), have been realized.

The ASM, however, gradually advanced as a supplemental payload. Ariel-ASM, with pin-hole cameras, operated successfully for seven years with the main payload, which made spectrum observations of bright X-ray sources (Holt 1976). In 1987 the ASM aboard the Japanese satellite Ginga (Tsunemi et al. 1989) succeeded the Ariel-ASM. Ginga-ASM was able

---

* Present Address: Research Institute for Science and Engineering, Waseda University, 3-4-1, Okubo, Shinjuku, Tokyo 169-8555.

to observe the spectra of X-ray novae as it scanned the sky from 60° through 360° once every day with multi-slat collimators. Ginga-ASM greatly advanced the science of black-hole binaries with the discovery of nova-like black-hole binaries (Tsunemi et al. 1989; Kitamoto et al. 1992; Kitamoto et al. 2000). Ginga-ASM was successfully operated for 4.5 years, and some of transients discovered by ASM were observed in detail by the main large-area counters aboard Ginga (Turner et al. 1989).

Since 1996, RXTE-ASM (a NASA satellite) has monitored known X-ray sources in addition to X-ray novae and transients (Levine et al. 1996). Systematic long-term data of Galactic variable sources provide quasi-periodic properties of the accretion disc (Zdziarski et al. 2007a, 2007b). RXTE-ASM has provided much useful data for X-ray variable sources for 13 years, but the detection limit is around 10 mCrab. Therefore, the main targets of RXTE-ASM were Galactic X-ray sources, of which monitoring was suitable for performing detailed observations of these targets with an RXTE prime instrument, a large-area proportional counter array (Remillard & McClintock 2006).

We now have long-term light curves for bright X-ray sources from the above-mentioned three ASMs. Some sources have revealed periodic or quasi-periodic components of long time scale with combined analyses over the last 30 years (Paul et al. 2000). Future ASMs taking over the three ASMs can continue to investigate further long-term behaviour of X-ray sources. Although the above-mentioned three ASMs have been in operation, they cannot adequately monitor AGNs because of their low sensitivity. Thus far, Galactic X-ray novae and transients data have been accumulated, although the information is not completely clear. No long-term variability of AGN has been observed with sufficient data. Therefore, the most important role for future ASMs is to achieve better the detection limits for AGN monitoring. Considering this historical situation, MAXI was proposed as a payload of ISS (Matsuoka et al. 1997). It will be one of the ASMs responsible for AGN monitoring. A slit-hole camera with a large detection area meets this requirement. Since MAXI has a composite structure of slit holes and slat collimators without a mirror system, the angular resolution is not good (i.e., the FWHM of slat collimators is 1°.5), but the localization accuracy can be 0°.1 for sources of sufficient statistics (e.g., bright sources and sources with enough counts accumulated for optimum time). A mirror-type ASM, such as the Lobster-eye ASM, is promising for the future, although its energy band is limited to soft X-rays (Priedhorsky et al. 1996).

The MAXI to be attached to the Japanese Experiment Module (JEM; Kibo) on the ISS is ready to be launched. In this paper we present an overview of MAXI and the new scientific contributions expected of it. The first part of this paper considers the astronomical science expected of MAXI. The second part describes the MAXI instrumentation, and observational simulations.

2. Key Science

The MAXI mission enables the investigation of ASMs and surveying. MAXI will alert astronomers of GRBs, X-ray novae, and flare-up increases of X-ray sources if they occur. Long-term data of X-ray sources will enable us to determine a special time scale of variability, e.g., long-term periodic or quasi-periodic motions of X-ray sources. MAXI can promote multi-wavelength observations in collaboration with other space and ground observatories, such as X-ray, infrared, and optical satellites, radio, and optical ground observatories. MAXI systematic observations of the variable activity of black-hole binaries and AGNs are used to investigate how and where they produce their variable activities.

MAXI provides unbiased X-ray source catalogues over all of the sky. Monthly or biannual X-ray catalogues could contribute to the long-term study of the variable behavior of AGN for the first time. A catalogue accumulated for two years could provide all-sky AGNs corresponding to a moderately deep survey of the entire sky. This unbiased AGN catalogue will far surpass an investigation of the distribution and evolution of AGNs for the HEAO-1 A2 catalogue, which has been utilized for a long time (Piccinotti et al. 1982). MAXI is also able to make an all-sky X-ray map with soft X-rays and medium-energy X-rays. The soft X-ray map provides line features, such as Oxygen X-ray lines, which are useful in researching geo-coronal recombination lines (Fujimoto et al. 2007) as well as the evolution of hot gas in the Galaxy (McCammon & Sanders 1990; Tanaka & Bleeker 1977).

The current Swift (Gehrels et al. 2009; Burrow 2009) and INTEGRAL (Ubertini et al. 2009) satellites with wide FOVs of hard X-ray detectors have provided X-ray source catalogues including AGNs in addition to a considerable number of transients. Since these results are complementary to those of MAXI, it could be promising to science that these three ASM missions will operate simultaneously. Furthermore, the recently developed gamma-ray large-area space telescope, the Fermi Gamma-Ray Space Telescope (Abdo et al. 2008; Thompson et al. 2009), is a gamma-ray ASM with an energy band complementary to that of MAXI. All-sky images with both ASMs may reveal new information.

2.1. X-Ray Novae and GRBs Alert

More than 90% of black-hole candidates are X-ray transients or novae (McClintock & Remillard 2006). In the last 20 years, 29 have been discovered, mostly with RXTE-ASM and partly with Ginga-ASM, while about 30% of them have been serendipitously discovered by pointing observatories (Negoro 2009). Thus far, observed X-ray novae are located near the galactic center and near the solar system; i.e., their distances are within about 6 kpc. Distant X-ray novae appear to be weak, but MAXI could detect these weak sources, since it can observe X-ray novae from distant regions about three times as far. Thus, it is expected that the nova discovery rate may increase by one order of magnitude.

X-ray light curves with energy spectra of X-ray novae have provided instability and phenomena deviating from the standard accretion-disc model (Tanaka & Shibazaki 1996). Data of both low and high luminosities have resulted in the creation of a new theory concerning accretion discs (Mineshige et al. 1994), but these samples are not enough. We also expect that MAXI could observe X-rays from classical novae. Multi-wavelength observations of classical novae could provide

useful information about the bursting mechanism of classical novae. Although classical novae are faint and soft in the X-ray band, the durations are of months to years (Mukai et al. 2008). Thus, MAXI could detect some of them.

Swift has discovered many GRBs, and has consequently enabled us to make rapid follow-up observations of them. Nevertheless, the energy band of the Swift detector is 15 to 200 keV (Gehrels et al. 2004). MAXI can cover the soft X-ray band of GRBs, and this information is important for understanding X-ray rich GRBs and X-ray flashes. It is expected that the population of the X-ray rich GRB is comparable to that of the GRB with an ordinary energy band (Sakamoto et al. 2005). The instant FOV of MAXI is not large, and thus MAXI will be able to detect 3.5 prompt emissions and 2.5 X-ray afterglows of GRB per year (Suzuki et al. 2009).

MAXI is also able to observe transient X-ray binary pulsars with high orbital eccentricity and transient low-mass X-ray binaries with neutron stars. Furthermore, Anomalous X-ray Pulsars (AXPs) are still enigmatic objects that appear as Soft Gamma Repeaters (SGRs) with enormous flux during a short time (Nakagawa et al. 2009; Morii 2009). Considering the recent Swift discovery of a new SGR (Barthelmy et al. 2008; Enoto et al. 2009), we could even expect MAXI to detect additional SGRs with weaker flux. Thus, MAXI may reveal a new frontier of AXPs (i.e., magnetars) by detecting numerous new magnetar candidates (Nakagawa et al. 2009). Recently, special interest concerning long type-I X-ray bursts has arisen with rare events of carbon-fueled super bursts and helium-fueled intermediately long bursts. These bursts are promising for investigating the deeper neutron star envelope (Keek & in't Zand 2008; Keek et al. 2008). MAXI may discover such rare occurrences of X-ray bursts.

2.2. Long-Term Variability of X-Ray Sources

Most X-ray sources with compact objects are variable, due to the instability of the accretion disc, and other reasons. Periodic or quasi-periodic long-term variability is sometimes created from interactions between the accretion disc and the binary system. If there were a third object in the X-ray sources, we could expect some other periodicity in addition to the binary period (Zdziarski 2007a). Such a third body might be useful for inspecting the accretion disc. However, no one has discovered such a triple-body system in X-ray sources. A composite time scale of variability would help to generate this knowledge, and/or may create new knowledge. An unusual X-ray transient from the galactic center region (Smith et al. 1998) is progressing in a new class of recurrent and fast X-ray transient sources (i.e., SFXTs). These transients sometimes occur in high-mass X-ray binaries associated with super-giant companions. It is promising for further investigations that MAXI, in addition to INTEGRAL and Swift, monitors these objects with a wide FOV (Ebisawa 2009; Ubertini et al. 2009). Generally, a time scale of variability of AGNs or supermassive black holes is longer than that of X-ray binaries. Non-recurrent X-ray flares on time scale of days have been observed from several non-active galaxies since ROSAT survey (e.g., Komossa 2002). Tidal disruption of a star by a supermassive black hole (Ress 1998) is the favored explanation of these unusual events. These might be also detected by the soft X-ray camera of MAXI

although very soft and weak.

2.3. Multi-Wavelength Observations of Variable Objects

The knowledge of bursts, transients, and variable objects has progressed considerably with multi-wavelength observations. Research of GRB afterglows has advanced greatly as a result of rapid follow-up observations in X-ray, optical, and radio bands (Gehrels et al. 2004), but there are still just a few samples of short GRBs and X-ray rich GRBs. Coordinate observations of Blazars in radio, infra-red, optical, X-ray, and ultra-high-energy (TeV) gamma-rays have confirmed a Synchrotron Self-Compton (SSC) model for highly variable periods (Kubo et al. 1998; Kataoka et al. 1999; Takahashi et al. 2000). However, the emission mechanism of other AGNs as well as Blazars has not yet been completely understood because of complicated correlations among multi-wavelength observations to help investigate this mechanism (Maoz et al. 2002). TeV gamma-ray observations by Ćerenkov telescopes have progressed remarkably since TeV gamma-rays from some Blazars were detected (Petry et al. 1996; Aharonian et al. 1997). GeV gamma-ray observations by Fermi-GLAST are now available as an ASM (Thompson et al. 2009). MAXI can promote further simultaneous multi-wavelength observations of Galactic active objects as well as AGNs with gamma-rays (GeV & TeV) to radio bands (Fender 2009; Madjeski et al. 2009).

2.4. Unbiased X-Ray Source Catalogues

The nominal beam size (i.e., angular resolution by FWHM) of MAXI is $1°\!.5 \times 1°\!.5$. It is estimated that the confusion limit of X-ray sources is $5 \times 10^{-12} \, \mathrm{erg \, cm^{-2} \, s^{-1}}$ from a recent $\log N$–$\log S$ plot of X-ray sources (Ueda et al. 2003); i.e., 0.2 mCrab in the energy band of 2 to 20 keV. Thus, we can set a detection limit of 0.2 mCrab as an ideal goal, although the period of its achievement depends on the intrinsic background and the systematic error. To estimate the observation time we conducted a realistic MAXI observational simulation. MAXI achieved a detection limit of 0.2 mCrab with a two-year observation (Ueda et al. 2009). Other simulations suggest that it is possible to detect 20 mCrab for one orbit (90 min), 4.5 mCrab for one day, and 2 mCrab for one week (Hiroi et al. 2009; Sugizaki et al. 2009). Some regions in the sky are covered by a bright region from the Sun, and are sometimes affected by the South Atlantic Anomaly (SAA). Therefore, detection sensitivities are estimated under the best condition. The detectability of MAXI is not uniform in the entire sky, but slightly depends on the direction. The MAXI simulation indicates that we can obtain 30–40 AGNs every week (Ueda et al. 2009). This sample is comparable to the number from HEAO 1-A2 (Piccinotti et al. 1982). We are also able to estimate about 1000 AGNs with two-year observations. MAXI observes those AGNs in a harder energy band than observed by ROSAT. Thus, MAXI could give an unbiased population ratio of Type I and Type II AGNs. Furthermore, if weekly or monthly catalogues are created, we can discover the intensity variability for a considerable number of AGNs. It would be possible to detect a flare-up of Blazars, and to then follow their light curves. The time sequence of X-ray unbiased catalogues is very useful for researching the evolution of AGNs as well as their long-term variability. Here,

the next comment is noted. Although much deeper surveys of AGNs in the 2–10 keV band with ASCA (e.g., Ueda et al. 1999) and Chandra / XMM-Newton (Brandt & Hasinger 2005 and references therein) have presented $\log N$–$\log S$ plots for researching the evolution of AGNs, they are limited to a small portion of the sky, and hence cannot constrain that of bright AGNs with small surface densities.

2.5. *Diffuse Cosmic X-Ray Emissions*

The problem of the diffuse cosmic X-ray background (CXB) has a long history. A recent deep survey of X-ray sources in a medium energy band of 2 to 10 keV (Ueda et al. 2003) suggests that the CXB may be due to the superposition of AGNs, as proposed theoretically (Morisawa et al. 1990). It is still unknown how some kinds of AGNs are distributed in the universe. The global CXB distribution could be compared with that of optical AGNs and/or an infrared map. Thus, we can investigate the evolution or emission mechanism of the all-sky AGN distribution. If we can obtain some difference in the distribution in different energy bands, we can investigate the distribution of Type I and Type II AGNs.

The diffuse emission of soft X-rays less than 1 keV is attributed to geo-coronal gas as well as hot bubbles from supernova remnants (Tanaka & Bleeker 1977; McCammon & Sanders 1990). ROSAT obtained a precise all sky map with a broad energy band of soft X-rays. MAXI can also obtain all-sky maps of soft X-rays but with better energy resolution (e.g., resolving Oxygen K-line, and Neon K-line). Recent Suzaku observations have revealed a strong contribution of recombination K-lines of oxygen and carbon in the geo-coronal region (Fujimoto et al. 2007). MAXI is able to observe the oxygen line with a seasonal variation and solar activity. Therefore, MAXI observations make it possible to discriminate between the contribution of the geo-corona and that of supernova remnants. Thus, we could investigate geo-coronal science as well as element-evolution of supernova remnants from soft X-ray line observations.

3. MAXI Project

The large-scale Space Station (SS) project started in 1985 with the collaboration of the USA, Japan, Canada, and the European Space Agency (ESA). Planning of the JEM was also initiated at that time. In 1995, Russia began to take part in the SS project. The project was subsequently reduced to its present scale, and then renamed the International Space Station (ISS). JEM planning and designing have continued, but actual construction and basic tests of the engineering model began at that time. JEM consists of a pressurized module for microgravity experiments and an exposed facility (EF).

ISS rotates synchronously in its orbit so that one side always points towards the center of the Earth, and the opposite side views the sky. Therefore, the sky side of JEM-EF surveys a great circle every ISS orbit. Themes for JEM-EF include the space science payload for astrophysics and Earth observations, and space technology experiments, such as robotics. However, JEM-EF does not provide a perfectly stable platform because of unknown factors of some attitude fluctuation. The payload size and weight are limited to the capacity of the
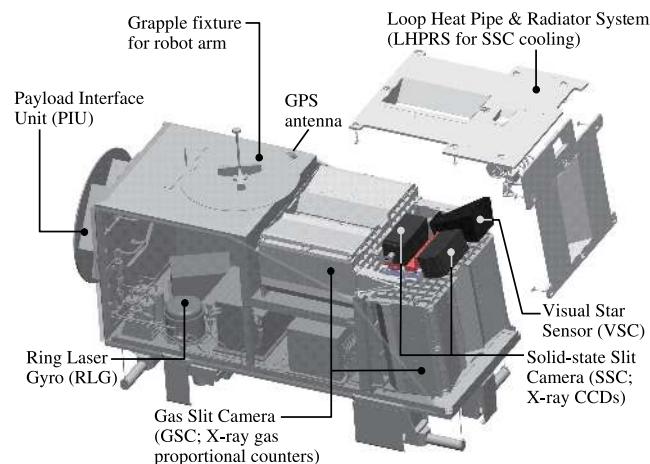

Fig. 1. Overview of MAXI; major subsystems are indicated.

JEM-EF. A payload can be suitable for survey observations, but not for pointing. Although a considerably wide FOV is available, the ISS structure and solar paddle partially block the view of JEM-EF. Since the ISS carries various experimental instruments and payloads, each instrument and payload has to accommodate many interfaces. Resources such as communication and power for each experiment or payload are also limited.

Considering these problems, MAXI was proposed and finally accepted in 1997 by the National Development Space Agency of Japan (NASDA), now known as the Japan Aerospace Exploration Agency (JAXA). Thus, MAXI is the first astronomical payload for JEM-EF aboard ISS. Although the launch was scheduled for 2003, the space shuttle, Columbia accident, and the ISS construction delay resulted in a postponement of the MAXI launch by several years. The MAXI science instruments consist of two types of X-ray cameras, the Gas Slit Camera (GSC) and the Solid-state Slit Camera (SSC). These instruments and the support instruments on the MAXI payload are shown in figure 1, and their characteristics are listed in table 1. The support instruments consist of a Visual Star Camera (VSC), a Ring Laser Gyroscope (RLG), a Global Positioning System (GPS) and a Loop Heat Pipe and Radiation System (LHPRS). The VSC and the RLG determine the directions of the GSC and the SSC as precisely as a few arc-seconds every second. The GPS attaches the absolute time as precisely as 0.1 ms to GSC photon data. The LHPRS is used for heat transportation and heat radiation from thermo-electric coolers (Peltier elements) to cool the CCD.

The main role of the GSC is to perform as an X-ray ASM, which has the best detectability than previous ASMs have for a time scale longer than hours. All-sky X-ray images obtained by GSC are also useful for new X-ray variable catalogues. On the other hand, the main mission of SSC is to make all-sky X-ray maps for extended sources with better energy resolution than ROSAT maps, although the detection area and live time for discrete sources are less by 1/20 than those of GSC. We also expect to detect transients in the soft X-ray band, although the detectability of transients with SSC is also poorer by 1/20 than that of GSC.

MAXI will be carried by the Space Shuttle, Endeavour,

Table 1. Specification of MAXI slit cameras.

	GSC[†]: Gas Slit Camera	SSC[†]: Solid-state Slit Camera
X-ray detector	12 pieces of one-dimensional PSPC; $Xe + CO_2$ 1 %	32 chips of X-ray CCD; 1 square inch, 1024×1024 pixels
X-ray energy range	2–30 keV	0.5–12 keV
Total detection area	5350 cm^2	200 cm^2
Energy resolution	18% (5.9 keV)	$\leq$ 150 eV (5.9 keV)
Field of view*	$1°\!.5 \times 160°$	$1°\!.5 \times 90°$
Slit area for camera unit	20.1 cm^2	1.35 cm^2
Detector position resolution	1 mm	0.025 mm (pixel size)
Localization accuracy	$0°\!.1$	$0°\!.1$
Absolute time resolution	0.1 ms (minimum)	5.8 s (nominal)
Weight[‡]	160 kg	11 kg

* FWHM × Full-FOV.

[†] MAXI total weight: 520 kg.

[‡] GSC consists of 6 camera units, where each unit consists of two PCs. SSC consists of two camera units, SSC-Z and SSC-H.

along with the JEM (or Kibo)-EF from Kennedy Space Center in the middle of 2009. MAXI will finally be mounted on JEM-EF within two weeks of Endeavour launch. At that time all of Kibo's modules will have been installed on ISS. After the basic arrangement of the structure and infrastructure of JEM, MAXI will conduct performance tests for about three months. MAXI has a nominal lifetime of two years, but the expected goal is five or more years to achieve long-term monitoring.

MAXI data will be down linked through the Low Rate Data Link (LRDL; MIL1553B), and the Medium Rate Data Link (MRDL; Ethernet). MAXI is operated through the Operation Control System (OCS) at Tsukuba Space Center (TKSC), JAXA. MAXI data are not only processed and analyzed at TKSC, but they are also transferred to the Institute of Physical and Chemical Research (RIKEN) MAXI data facility. General users of MAXI can request scientific data from RIKEN (a main port) as well as from JAXA (a sub-port) whenever they desire. To search where X-ray novae, transients, or flaring phenomena appear suddenly in the sky we will conduct automatic data analysis at TKSC by using down-linked data from LRDL. If such a source is discovered, we will report this event to astronomers and dedicated users worldwide via the Internet from TKSC. This nova alert system has been developed to achieve automatic alerts (Negoro et al. 2008). The MAXI team will also maintain archival data at RIKEN using the data from LRDL and MRDL, such as all-sky X-ray images, X-ray light curves, and spectra of dedicated X-ray sources. In principle, all astronomical data of MAXI will be available for public distribution (Kohama et al. 2009).

4. X-Ray Mission Instruments

A specific object is observed by MAXI with a slit camera for a limited time during every ISS orbit. The X-ray detector of the camera is sensitive to a one-dimensional image through the slit, where the wide FOV through the slit spans the sky perpendicular to the ISS moving direction, as shown in figure 2. A scanning image of an object is obtained with the triangular response of a slat collimator according to the ISS movement. An intersection of the slit image and the triangular response
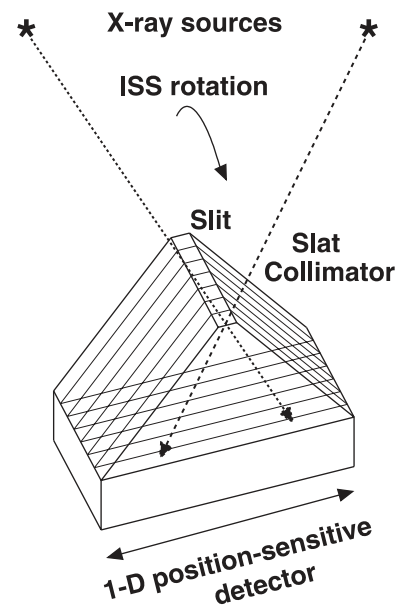

Fig. 2. Principle of the MAXI Slit Camera; it consists of slit & slat collimators and a one-dimensional position sensitive X-ray detector.

image corresponds to a source location in the sky as a Point Spread Function (PSF). This is shown in figure 3.

Objects located along a great circle stay for 45 s in the FOV of the MAXI cameras, where the time of stay is the shortest in the MAXI normal direction (for a great circle). For objects in the slanted field from the great circle, they achieve a slightly longer observation. Any target will come repeatedly in each field of the horizontal and zenithal cameras with every ISS orbital period. In this situation MAXI can intermittently monitor a short-time scale variability for bright X-ray sources, such as X-ray pulsars and low-mass X-ray binaries. It can monitor their variability of weak sources on a time scale of 90 min or longer if we integrate the data. MAXI has two types of X-ray cameras: the GSC and the SSC, which are described in the following subsection.
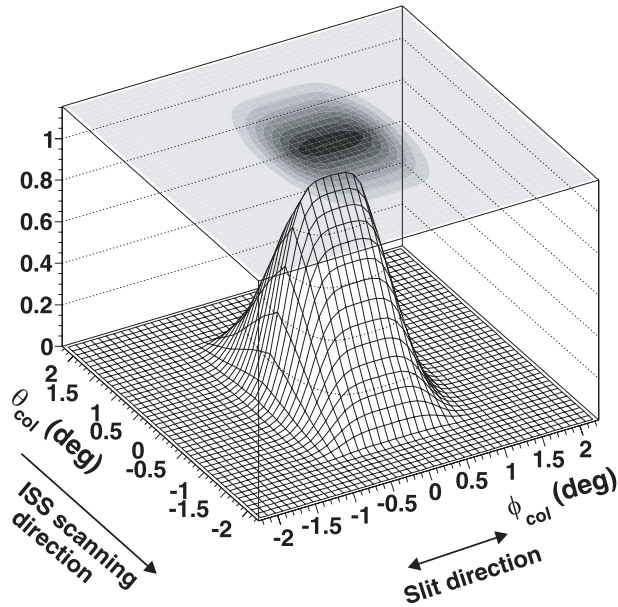
Fig. 3. Typical sample of PSF (Point Spread Function); a slat collimator has a triangular response (ISS scanning direction), while a slit collimator has a trapezoidal response (the slit direction corresponding to β in figure 6).
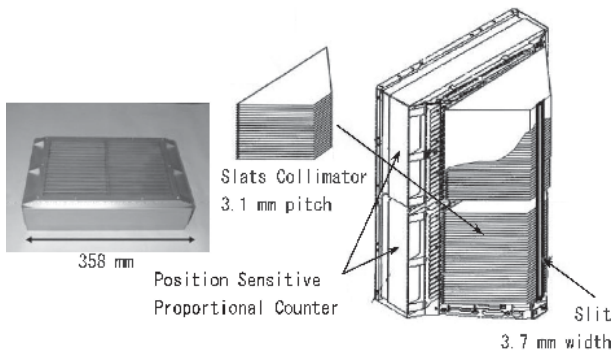

Fig. 4. GSC unit and a gas-proportional counter; the unit consists of two gas-proportional counters, slit & slat collimators.

4.1. Gas Slit Camera (GSC)

GSC is the main X-ray camera, and consists of six units of a conventional slit camera, as shown in figure 1 and table 1 (Mihara et al. 2009). The GSC unit consists of two one-dimensional proportional counters (produced by Oxford Instruments Co. in Finland), and slit & slat collimators, as shown in figure 4. Thus, twelve proportional counters have a $5350 \, cm^2$ detection area in total. Each counter has six cells of resistive carbon wires that are guarded by a veto-detector region in the bottom and on both sides (Mihara et al. 2002), while a carbon wire divides the charge from the signal into both terminals for one-dimensional determinations. The X-ray detection efficiency of the proportional counter (Xe 1.4 atmospheres with 1% CO_2) is plotted against X-ray energy in figure 5. The observational energy band of GSC is set to be 2–30 keV in the standard operation mode where the detection
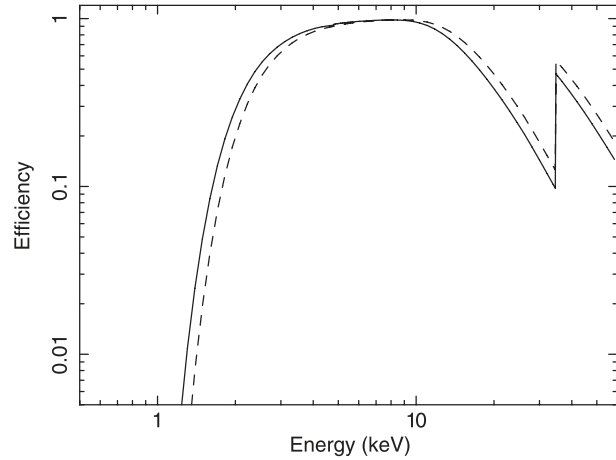

Fig. 5. X-ray detection efficiency of the MAXI proportional counter for energy; a solid line indicates the efficiency for normal-incident X-rays, while a dashed line indicates that of incident X-rays from $40°$.

efficiency for X-rays in this band is above 10%, as shown in figure 5. The observation above the Xe K-edge of 34.6 keV is possible as a special mode by adjusting the amplifier gain and the high voltage. Although a response function above the Xe K-edge is complicated, due to the escape peak, a test for this function has been performed using synchrotron X-ray beams. The slat collimator response is $3°.5$ in bottom-to-bottom, and a slit image corresponds to $1°.5$, covering a wide field of between $−40°$ and $+40°$. The proportional counters detect incident X-ray photons from the vertical to the $±40°$ slant direction.

Two FOVs of GSC-H and GSC-Z are placed in the horizontal (forward) and zenithal directions to compensate when the sky is unobservable to one FOV or the other (due to high radiation background, such as SAA). The FOV of one camera is $80°$. Two camera units can cover $160°$, but the FOV of each central camera of GSC-H and GSC-Z overlaps with each half of the FOV of both side cameras to even the exposures, as shown in figure 6, which shows the product of the effective area and the dwell time according to one orbit scan. The exposure time per orbit depends on the direction of a star by a factor of $1/\cos\beta$, where β is the angle of the star slanted from scanning a great circle. Both edges of $10°$ in this figure are omitted, due to a shadow of the ISS structure, where the scanning loss is 1.5%. The forward FOV is tilted up by $6°$ so as not to observe Earth even when the ISS attitude changes. Thus, the FOV of GSC-H can scan the sky with ISS rotation without Earth occultation. By making the observation time longer than 90 min, we made the instrument simpler, and then optimized it to search in the AGN discovery space for a longer-term AGN variability (> 1.5 hr).

Considering this directional performance, we conducted various laboratory tests of all proportional counters. Here, we explain some of the results. The position resolution was tested at every 2 mm segment of two-dimension on the incident window for all proportional counters. The data were taken using 0.1 mm pencil X-ray beams with X-ray energies of 4.6, 8.0, and 17.4 keV. The total length of the carbon anode wire is
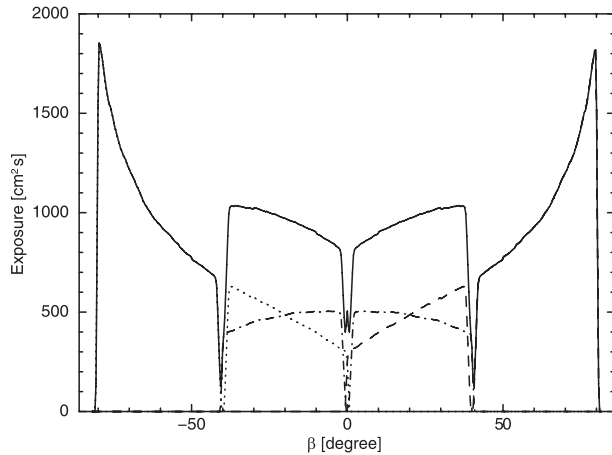
Fig. 6. The solid line shows the total product of effective area and dwelt time according to one orbit scan for a point source for the angle (β) slanted from scanning a great circle. This value is common to GSC-Z and GSC-H. The chain line indicates the contribution of a central GSC unit only, while the dashed line and the dotted line are those of the right side GSC unit and the left side GSC unit only, respectively.

32 cm; thus, the total resistance is 31 to 37 kΩ. The difference in the resistance depends on a slight difference of the wire diameters. The energy response also differs for different anode wires. We took comprehensive data useful for the energy response and the position response (Mihara et al. 2002; Isobe et al. 2004). We also took slat collimator response data using X-ray pencil beams (Morii et al. 2006). The data-base, including all of these data, is regarded as being the response function at the time of data analysis. In actual data analysis, we will use each response function for the two-dimensional surface of all carbon wires. The pulse-height response depends on the X-ray energy, where hard X-rays suffer the effect of anomalous gas amplification (Mihara et al. 2002).

The simultaneous background for a localized source is measured in two regions separated from the source on the same detector in the FOV direction. Another background is measured in two regions just before and after observing the source on the scanning path, where the two regions are separated from the source. In this case, both measurement locations of the background on the detector are the same as the measurement location on the detector of the source. The background is employed if there are no appreciable sources in these directions. In addition, intrinsic background is necessary to obtain the cosmic diffuse background. The intrinsic background is gradually changing in orbit, and for a time even in the same direction (Hayashida et al. 1989). There is the small portion covered by a window frame of each detector in which cosmic diffuse X-rays as well as source X-rays are never irradiated. A small portion of the North Pole direction is also shadowed by the ISS structure. Although these intrinsic background count rates are not enough to measure for an instant of time, the data accumulated for days or more could be used to make a reasonable model of the intrinsic background, as obtained for Ginga proportional counters (Hayashida et al. 1989).
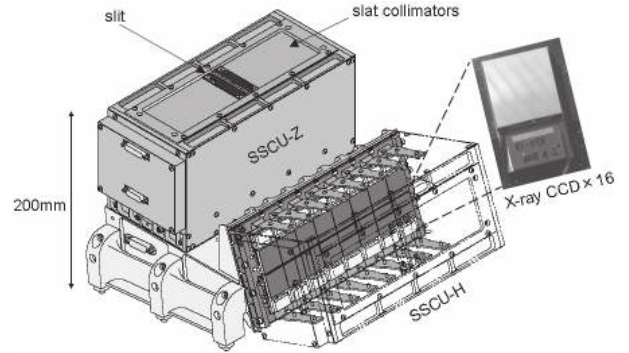

Fig. 7. SSC consisting of a horizontal SSC (SSC-H) and a zenithal SSC (SSC-Z), and a CCD chip is depicted separately.
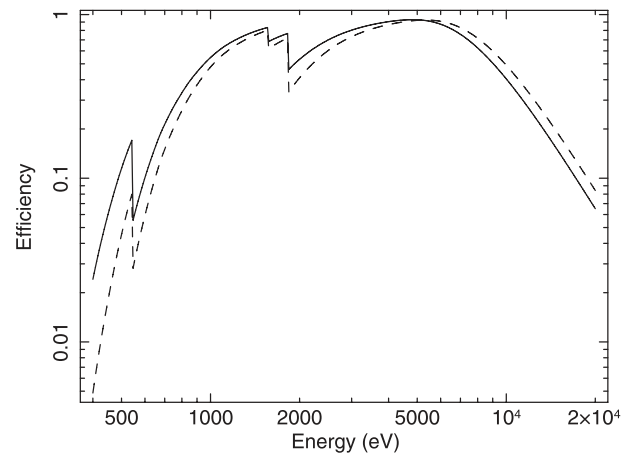

Fig. 8. X-ray the detection efficiency of MAXI CCD for energy; the solid line is the efficiency for a normal-incident X-ray, while the dashed line indicates that for X-rays incident from 40°.

4.2. Solid-State Slit Camera (SSC)

Each unit of SSC-H/Z consists of 16 CCDs, where each CCD acts as a one-dimensional position-sensitive detector for the slat collimator and the slit hole, similar to that of the GSC system presented in figure 1 and table 1 (Tomida et al. 2009). The SSC-H camera is tilted up 16° so as not to view the upper atmosphere. The response of the slat collimator scanning direction is 3° for bottom-to-bottom, while a slit image corresponds to 1°.5, covering a wide FOV of 90°, as shown in figure 7. One orbit scan of the SSC corresponds to 90° × 360°. Thus, it takes SSC 70 days to scan the entire sky, depending on the precession of the ISS orbital plane, except for the bright region around the Sun. Thus, SSC will acquire actual all-sky images every half year.

The X-ray CCD chip of SSC is produced by Hamamatsu Photonics K.K. The CCD depletion layer is about 70 μm, of which the X-ray detection efficiency is indicated in figure 8. The observation energy band of SSC is set to be 0.5–12 keV in the standard mode, but observations above 12 keV are possible in a special mode. However, since SSC is characterized by

a low-energy band, the energy band may be slightly shifted to a lower energy than 0.5 keV, depending on the temperature for thermal noise. The CCD with 1024×1024 pixels, and a pixel size of $24\,\mu m \times 24\,\mu m$ is a two-dimensional array, but SSC requires only one-dimensional position information. Hence, multiple rows are summed in a serial register at the bottom of the imaging region, and the summed charges in the serial register are transferred to a read-out node. 8, 16, 32, or 64 summed rows can be selected in normal observations by commands. The larger is this number, the better is the time resolution, and the better is the angular resolution in the X-ray sky map.

The CCD is sensitive to particle radiation, but an irradiation test of the simulated radiation belt fluence suggests that the CCD can survive for the expected three-year mission (Miyata et al. 2003). Furthermore, it is possible to inject charges in the CCD before it becomes damaged due to irradiation (Miyata et al. 2003). Charge-injection effectively restores the degraded performance of X-ray CCDs (Tomida et al. 1997).

To achieve better energy resolution with a CCD, all CCDs are cooled to $-60°C$ using thermo-electric coolers (Peltier devices) and the LHPRS. The maximum power of the thermo-electric cooler is 1 W/CCD. The LHPRS can automatically transfer heat from the Peltier device, and emit heat from the radiation panel. Performance tests in the laboratory have been satisfactorily conducted (Miyata et al. 2002; Katayama et al. 2005). The nominal energy resolution width of X-ray spectra is 150 eV for Mn K X-rays (5.9 keV).

4.3. Support Sensor

Since the ISS has a huge structure of ~ 108 m and ~ 420 tons, the attitude determined in a certain part of the ISS may be slightly different from that in a distant part, due to shaking of the structure. MAXI is designed to determine a target location as precisely as less than $0°1$ Thus, it is necessary to determine the attitude of the MAXI coordinate by less than $0°1$ every time. For this purpose, MAXI, itself, has a VSC and an RLG. The VSC can observe three or more stars, and it can determine a MAXI coordinate by $0″1$. When the VSC is not available for a measurement due to solar radiation, the RLG will extrapolate the attitude from a certain result of the VSC to the following result. This attitude determination is performed automatically by onboard software including a Kalman filter on the MAXI data processor (Ueno et al. 2009; Horike et al. 2009).

The high voltage of a proportional counter of GSC will be reduced to 0 V when solar radiation or SAA radiation is extremely strong. The command signal for this reduction will be issued by working of the Radiation Belt Monitor (RBM). This high-voltage reduction is also useful for setting program commands in advance, because of possible predictions of the solar position and the SAA location.

The time precision of photon acquisition from GSC is 0.1 ms by referring to GPS signals. This precise absolute time is used for milli-second pulsars and burst acquisition analysis. Thus, only one GPS is installed in MAXI for precise time reference without any unknown lag. However, the time resolution of SSC is 5.8 s in the normal observation mode.

5. MAXI Simulation and Expected Performance

A realistic simulation has been conducted with the recently developed MAXI simulator, which generates fully simulated data of MAXI instruments on the ISS (Eguchi et al. 2009). The simulator takes into account various conditions on the ISS, i.e., the occultation of the sky with solar panels, particle and intrinsic background, and the response function of the X-ray cameras. The attitude data and absolute time are attached to each event data on the ground. Thus, we can plot each event with energy information in a certain direction in the sky. Integrated events from a certain direction for a certain time correspond to intensity, including background from the direction. Here, we demonstrate some of the simulated results (Hiroi et al. 2009; Sugizaki et al. 2009).

First, we consider the detectability of the GSC. Figure 9 illustrates one-orbit and one-week observations. The results indicate that we can detect a 20 mCrab source in one-orbit at a confidence level of 5-sigma, and a 2 mCrab source in one-week at a level of 5-sigma. These simulations are estimated for the energy band of 2–30 keV of the Crab nebula spectrum. This simulation is ideal, because the particle and intrinsic background of $10\,counts\,s^{-1}$ per counter steady, except for statistical fluctuation during the observation time, and this background is subtracted with the statistical fluctuation from integrated events of the source. The spectrum of an intrinsic background is referred to the laboratory test result. In reality, we must consider the changeable background on the ISS orbit and systematic errors for attitude determination and response functions. The final detectability could be 0.2 mCrab for a two-year observation, which means a source confusion limit for the angular resolution of $1°5$.

Here, it is noted again that the above 5-sigma detectability is under the best condition for a known source. The detectability depends on the intrinsic background or trapped particle background. Either of the zenithal and horizontal cameras can observe most directional sources, even if the ISS passes through the SAA. This makes the detectability uniform for most directions, except the direction around the Sun if observations are repeated by orbits. In fact, a deviation from uniformity of the detectability of one orbit becomes worse by about 65% for sources observed on the SAA path, while that of one day becomes uniform within 10%–20% for any direction, except for the solar region. We evaluated another detectability, excluding observation in the region less than the cut-off rigidity of 8 (e.g., aurora region). The situation of this detectability is not so much different from that of the aforementioned detectability. Lastly, it is noted that the detectability for an unknown source is not significantly different from that for known sources. The one-sigma location error for unknown 5-sigma sources is about $0°2$ for both one-day and one-week observations.

Second, we performed a simulation to derive the energy spectra of a source of 1 Crab for a one-orbit and a one-day observation, as shown in figure 10. This simulation is also ideal, because the background is steady only with a statistical fluctuation, and an ideal determination of the attitude without an unknown systematic error is assumed. Nevertheless, it is concluded that reasonable spectra from a considerable number
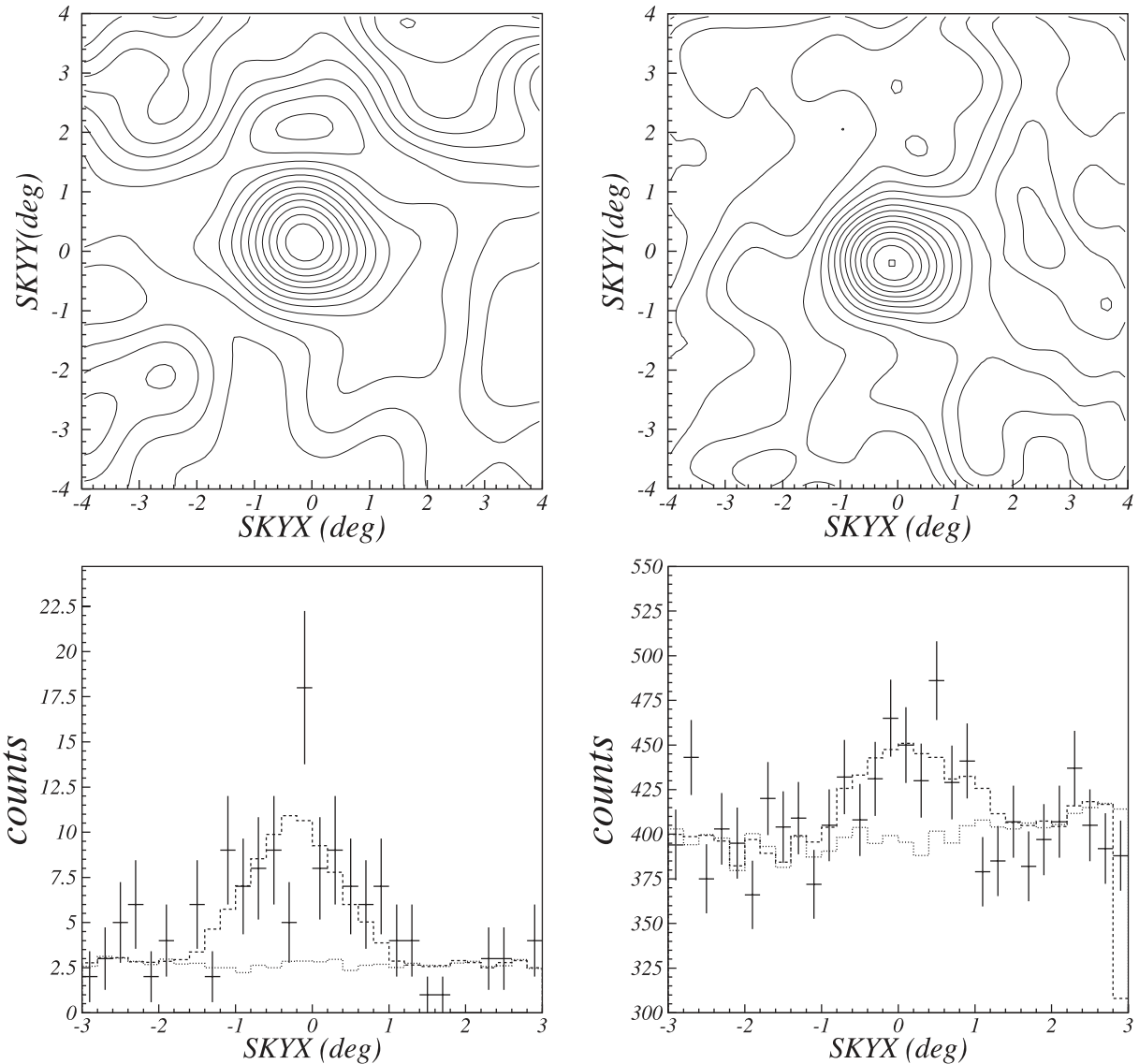
Fig. 9. (Left) Simulation used to detect a source of 20 mCrab for one ISS orbit. Contours are smoothed in the upper panel, while a cut figure through a peak is indicated with data points in the lower panel. (Right) Simulation used to detect a source of 2 mCrab in one week. Contours are smoothed in the upper panel, while a cut figure through a peak is indicated with data point in the lower panel.

of sources can be obtained by MAXI.

Another important goal of MAXI is to make X-ray source catalogues for every period of concern. We can make light curves with the time bin for various X-ray sources. The light curves of most galactic X-ray sources are obtained with time bins of one orbit or one day. If the time bin is one month, it is possible to make light curves of a considerable number of AGNs brighter than 1 mCrab, as shown in the lower panel of figure 11. It is not easy at a glance to discriminate between weak sources and the CXB, but 1–2 mCrab sources are significantly detected, as simulated in figure 9b. If we integrate all event data from the sky for two years, we can create an X-ray source catalogue brighter than 0.2 mCrab at a confidence level of 5-sigma. In general, since the time scale of the variability of AGNs is longer than that of galactic sources, catalogues with time bins of one month and one year will provide new

information about long-term variable sources, such as a super-massive Binary Black Hole (BBH). Actually, an all-sky image for every six-month observation is compatible with the result of HEAO-1 A2.

6. Concluding Remarks

MAXI is the first payload to be attached to JEM-EF (Kibo-EF) of the ISS. It consists of two kinds of X-ray cameras: the Gas Slit Camera (GSC), which has one-dimensional position sensitive gas-proportional counters with a 2 to 30 keV X-rays energy band, and the Solid-state Slit Camera (SSC), which has X-ray CCDs with a 0.5 to 12 keV X-rays energy band. MAXI will provide an all-sky X-ray image acquisition capability under the best conditions for every ISS orbit. If MAXI scans the sky for one week, it could make a 2 mCrab X-ray
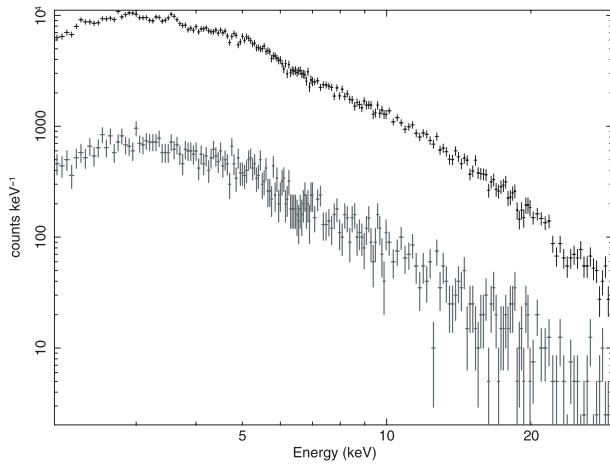
Fig. 10. Simulated spectra of Crab nebula for one-orbit (lower spectrum) and one-day (upper one) observations.

all-sky image, excluding the bright region around the Sun. Thus, MAXI will not only rapidly inform astronomers worldwide about X-ray novae and transients, if they occur, but also observe the long-term variability of galactic and extra-galactic X-ray sources. At the same time, MAXI will provide X-ray source catalogs accumulated for various periods such as six months, one and more years.

All MAXI instruments are ready for launch. Data processing and analysis software, including an alert system on the ground, are being developed by the mission team. MAXI will be attached to JEM(Kibo)-EF in mid-2009. Anyone can participate in follow-up or multi-wavelength observations of MAXI objects with ground optical and radio telescopes, and at space observatories. Please contact the present authors for more information and further collaboration.

Finally, please refer to the Proceedings of Astrophysics with All-Sky X-Ray Observations — 3rd International MAXI Workshop, RIKEN, Wako, Japan, June 10–12, 2008, ed.,
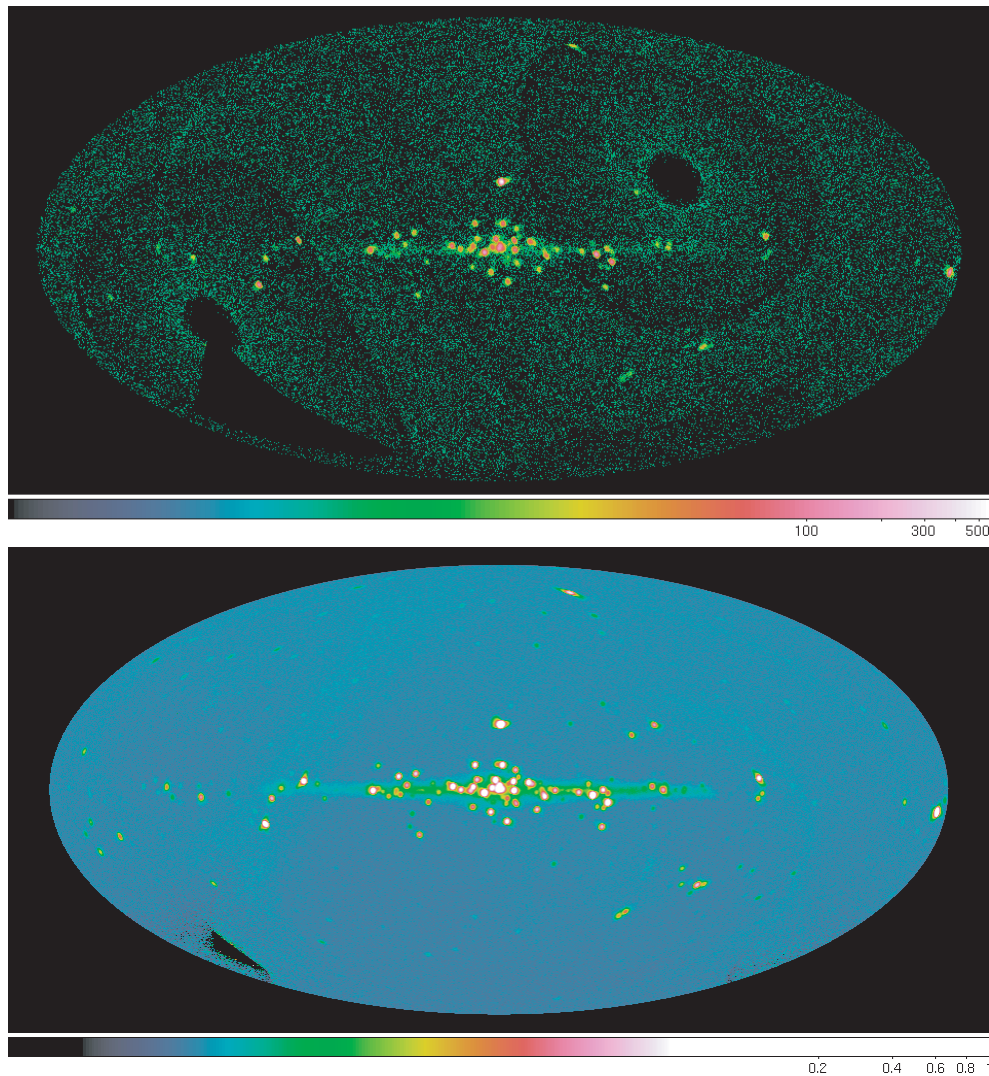

Fig. 11. An all-sky X-ray source image (raw data) simulated for one-orbit observation (upper panel) and an image (exposure corrected) for one-month (lower panel) on the galactic coordinate. The undetected (dark) region on the left bottom corresponds to the solar direction. The two circular dark regions on the upper panel correspond to unobservable regions around both end directions of the ISS pitch axis.

References

Abdo, A. A., et al. 2008, Science, 322, 1218

Aharonian, F., et al. 1997, A&A, 327, L5

Barthelmy, S. D., et al. 2008, Astronomer's Telegram, 1676

Brandt, W. N., & Hasinger, G. 2005, ARA&A, 43, 827

Burrow, D. 2009, in Proc. Astrophysics with All-Sky X-Ray Observations — 3rd international MAXI Workshop, ed. N. Kawai, T. Mihara, M. Kohama, & M. Suzuki, JAXA-SP-08-014E (Chofu, Tokyo: JAXA), 228

Costa, E., et al. 1997, Nature, 387, 783

Ebisawa, K. 2009, in Proc. Astrophysics with All-Sky X-Ray Observations — 3rd international MAXI Workshop, ed. N. Kawai, T. Mihara, M. Kohama, & M. Suzuki, JAXA-SP-08-014E (Chofu, Tokyo: JAXA), 82

Eguchi, S., Hiroi, K., Ueda, Y., Sugizaki, M., Tomida, H., Suzuki, M., & the MAXI team 2009, in Proc. Astrophysics with All-Sky X-Ray Observations — 3rd international MAXI Workshop, ed. N. Kawai, T. Mihara, M. Kohama, & M. Suzuki, JAXA-SP-08-014E (Chofu, Tokyo: JAXA), 44

Enoto, T., et al. 2009, ApJ, 693, L122

Fender, R. 2009, in Proc. Astrophysics with All-Sky X-Ray Observations — 3rd international MAXI Workshop, ed. N. Kawai, T. Mihara, M. Kohama, & M. Suzuki, JAXA-SP-08-014E (Chofu, Tokyo: JAXA), 76

Fujimoto, R., et al. 2007, PASJ, 59, S133

Gehrels, N., et al. 2004, ApJ, 611, 1005

Gehrels, N., & SWIFT Team 2009, in Proc. Astrophysics with All-Sky X-Ray Observations — 3rd international MAXI Workshop, ed. N. Kawai, T. Mihara, M. Kohama, & M. Suzuki, JAXA-SP-08-014E (Chofu, Tokyo: JAXA), 282

Hayashida, K., et al. 1989, PASJ, 41, 373

Hiroi, K., Ueda, Y., Eguchi, S., & MAXI team 2009, in Proc. Astrophysics with All-Sky X-Ray Observations — 3rd international MAXI Workshop, ed. N. Kawai, T. Mihara, M. Kohama, & M. Suzuki, JAXA-SP-08-014E (Chofu, Tokyo: JAXA), 54

Holt, S. S. 1976, Ap&SS, 42, 123

Holt, S. S., & Priedhorsky, W. 1987, Space Sci. Rev., 45, 269

Horike, N., Maeda, K., & Ueno, S. 2009, in Proc. Astrophysics with All-Sky X-Ray Observations — 3rd international MAXI Workshop, ed. N. Kawai, T. Mihara, M. Kohama, & M. Suzuki, JAXA-SP-08-014E (Chofu, Tokyo: JAXA), 24

Isobe, N., et al. 2004, in Proc. SPIE, 5165, X-ray and Gamma-ray Instrumentation for Astronomy XIII, ed. K. A. Flanagan, & O. H. W. Siegmund (Bellingham, WA: SPIE), 354

Kataoka, J., et al. 1999, ApJ, 514, 138

Katayama, H., Tomida, H., Matsuoka, M., Tsunemi, H., Miyata, E., Kamiyama, D., & Nemes, N. 2005, Nucl. Instrum. Methods Phys. Res., Sect. A, 541, 350

Keek, L., & in't Zand, J. J. M. 2008, in Proc. 7th INTEGRAL Workshop, 32

Keek, L., in't Zand, J. M. M., Kuulkers, E., Cumming, A., Brown, E. F. & Suzuki, M. 2008, A&A, 479, 177

Kitamoto, S., Egoshi, W., Miyamoto, S., Tsunemi, H., Ling, J. C., Wheaton, Wm. A., & Paul, B. 2000, ApJ, 531, 546

Kitamoto, S., Tsunemi, H., Miyamoto, S., & Hayashida, K. 1992, ApJ, 394, 609

Klebesadel, R. W., Strong, I. B., & Olson, R. A. 1973, ApJ, 182, L85

Kohama, M., et al. 2009, in Proc. Astrophysics with All-Sky X-Ray Observations — 3rd international MAXI Workshop, ed. N. Kawai, T. Mihara, M. Kohama, & M. Suzuki, JAXA-SP-08-014E (Chofu, Tokyo: JAXA), 40

Komossa, S. 2002, Rev. Modern Astron., 15, 27

Kubo, H., Takahasi, T., Madejski, G., Tashiro, M., Makino, F., Inoue, S., & Takahara, F. 1998, ApJ, 504, 693

Levine, A. M., Bradt, H., Cui, W., Jernigan, J. G., Morgan, E. H., Remillard, R., Shirey, R. E., & Smith, D. A. 1996, ApJ, 469, L33

Madjeski, G., Kataoka, J., & Sikora, M. 2009, in Proc. Astrophysics with All-Sky X-Ray Observations — 3rd international MAXI Workshop, ed. N. Kawai, T. Mihara, M. Kohama, & M. Suzuki, JAXA-SP-08-014E (Chofu, Tokyo: JAXA), 180

Maoz, D., Markowitz, A., Edelson, R., & Nandra, K. 2002, AJ, 124, 1988

Matsuoka, M., et al. 1997, in Proc. SPIE, 3114, EUV, X-Ray, and Gamma-Ray Instrumentation for Astronomy VIII, ed. O. H. Siegmund & M. A. Gummin (Bellingham, WA: SPIE), 414

McCammon, D., & Sanders, W. T. 1990, ARA&A, 28, 657

McClintock, J. E., & Remillard, R. A. 2006, in Compact Stellar X-ray Sources, ed. W. H. G. Lewin & M. van der Klis (Cambridge: Cambridge Univ. Press), 157

Mihara, T., et al. 2002, in Proc. SPIE, 4497, X-ray and Gamma-ray Instrumentation for Astronomy XII, ed. K. A. Flanagan & O. H. Siegmund (Bellingham, WA: SPIE), 173

---

[1] ⟨http://cosmic.riken.jp/maxi/astrows/⟩. This paper edition is published in JAXA Special Publication, JAXA-SP-08-014E, by JAXA, Chofu, Tokyo 182-8522

Mihara, T., et al. 2009, in Proc. Astrophysics with All-Sky X-Ray Observations — 3rd international MAXI Workshop, ed. N. Kawai, T. Mihara, M. Kohama, & M. Suzuki, JAXA-SP-08-014E (Chofu, Tokyo: JAXA), 14

Mineshige, S., Hirano, A., Kitamoto, S., Yamada, T. T., & Fukue, J. 1994, ApJ, 426, 308

Miyata, E., et al. 2002, Jpn. J. Appl. Phys., 41, 7542

Miyata, E., et al. 2003, Jpn. J. Appl. Phys., 42, 4564

Morii, M. 2009, in Proc. Astrophysics with All-Sky X-Ray Observations — 3rd international MAXI Workshop, ed. N. Kawai, T. Mihara, M. Kohama, & M. Suzuki, JAXA-SP-08-014E (Chofu, Tokyo: JAXA), 114

Morii, M., et al. 2006, in Proc. SPIE, 6266, Space Telescopes and Instrumentation II: Ultraviolet to Gamma Ray, ed. M. J. L. Turne, & G. Hasinger (Bellingham, WA: SPIE), 62663U

Morisawa, K., Matsuoka, M. Takahara, F., & Piro, L. 1990, A&A, 236, 299

Mukai, K., Orio, M., & Della Valle, M. 2008, ApJ, 677, 1248

Nakagawa, Y. E., Yoshida, A., & Yamaoka, K. 2009, in Proc. Astrophysics with All-Sky X-Ray Observations — 3rd international MAXI Workshop, ed. N. Kawai, T. Mihara, M. Kohama, & M. Suzuki, JAXA-SP-08-014E (Chofu, Tokyo: JAXA), 120

Negoro, H. 2009, in Proc. Astrophysics with All-Sky X-Ray Observations — 3rd international MAXI Workshop, ed. N. Kawai, T. Mihara, M. Kohama, & M. Suzuki, JAXA-SP-08-014E (Chofu, Tokyo: JAXA), 60

Negoro, H. et al. 2008, in ASP Conf. Ser., 394, Astronomical Data Analysis Software and Systems, ed. R. W. Argyle, P. S. Bunclark, & J. R. Lewis (San Francisco: ASP), 597

Paul, B., Kitamoto, S., & Makino, F. 2000, ApJ, 528, 410

Petry, D., et al. 1996, A&A, 311, L13

Piccinotti, G., Mushotzky, R. F., Boldt, E. A., Holt, S. S., Marshall, F. E., Serlemitsos, P. J., & Shafer, R. A. 1982, ApJ, 253, 485

Priedhorsky, W. C., & Holt, S. S. 1987, Space Sci. Rev., 45, 291

Priedhorsky, W. C., Peele, A. G., & Nugent, K. A. 1996, MNRAS, 279, 733

Rees, M. J. 1988, Nature, 333, 523

Remillard, R. A., & McClintock, J. E. 2006, ARA&A, 44, 49

Ricker, G., et al. 2002, ApJ, 571, L127

Sakamoto, T., et al. 2005, ApJ, 629, 311

Shirasaki, Y., et al. 2003, PASJ, 55, 1033

Smith, D. M., Main, D., Marshall, F., Swank, J., Heindl, W. A., Leventhal, M., in't Zand, J. J. M., & Heise, J. 1998, ApJ, 501, L181

Sugizaki, M., & MAXI Software Team 2009, in Proc. Astrophysics with All-Sky X-Ray Observations — 3rd international MAXI Workshop, ed. N. Kawai, T. Mihara, M. Kohama, & M. Suzuki, JAXA-SP-08-014E (Chofu, Tokyo: JAXA), 48

Suzuki, M., & MAXI Team 2009, in Proc. Astrophysics with All-Sky X-Ray Observations — 3rd international MAXI Workshop, ed. N. Kawai, T. Mihara, M. Kohama, & M. Suzuki, JAXA-SP-08-014E (Chofu, Tokyo: JAXA), 224

Takahashi, T., et al. 2000, ApJ, 542, L105

Tanaka, Y., & Bleeker, J. A. M. 1977, Space Sci. Rev., 20, 815

Tanaka, Y., & Shibazaki, N. 1996, ARA&A, 34, 607

Thompson, D, J., & the GLAST LAT Collaboration 2009, in Proc. Astrophysics with All-Sky X-Ray Observations — 3rd international MAXI Workshop, ed. N. Kawai, T. Mihara, M. Kohama, & M. Suzuki, JAXA-SP-08-014E (Chofu, Tokyo: JAXA), 288

Tomida, H., et al. 1997, PASJ, 49, 405

Tomida, H., et al. 2009, in Proc. Astrophysics with All-Sky X-Ray Observations — 3rd international MAXI Workshop, ed. N. Kawai, T. Mihara, M. Kohama, & M. Suzuki, JAXA-SP-08-014E (Chofu, Tokyo: JAXA), 18

Tsunemi, H., Kitamoto, S., Manabe, M., Miyamoto, S., Yamashita, K., & Nakagawa, M. 1989, PASJ, 41, 391

Tsunemi, H., Kitamoto, S., Okamura, S., & Roussel-Dupré, D. 1989, ApJ, 337, L81

Turner, M. J. L., et al. 1989, PASJ, 41, 345

Ubertini, P., & the IBIS Survey Team 2009, in Proc. Astrophysics with All-Sky X-Ray Observations — 3rd international MAXI Workshop, ed. N. Kawai, T. Mihara, M. Kohama, & M. Suzuki, JAXA-SP-08-014E (Chofu, Tokyo: JAXA), 276

Ueda, Y., et al. 1999, ApJ, 518, 656

Ueda, Y., Akiyama, M., Ohta, K., & Miyaji, T. 2003, ApJ, 598, 886

Ueda, Y., Hiroi, K., Eguchi, S., & the MAXI team 2009, in Proc. Astrophysics with All-Sky X-Ray Observations — 3rd international MAXI Workshop, ed. N. Kawai, T. Mihara, M. Kohama, & M. Suzuki, JAXA-SP-08-014E (Chofu, Tokyo: JAXA), 166

Ueno, S., et al. 2009, in Proc. Astrophysics with All-Sky X-Ray Observations — 3rd international MAXI Workshop, ed. N. Kawai, T. Mihara, M. Kohama, & M. Suzuki, JAXA-SP-08-014E (Chofu, Tokyo: JAXA), 8

Zdziarski, A. A., Gierliński, M., Wen, L., & Kostrzewa, Z. 2007b, MNRAS, 377, 1017

Zdziarski, A. A., Wen, L., & Gierliński, M. 2007a, MNRAS, 377, 1006